

Spontaneous solitons in stimulated Raman scattering

D. C. MacPherson, R. C. Swanson, and J. L. Carlsten

Physics Department, Montana State University, Bozeman, Montana 59717

(Received 25 September 1989)

It has been predicted that quantum fluctuations will lead to the formation of spontaneous solitons in stimulated Raman scattering. We present experimental data in support of this prediction. From an ensemble of 1000 shots we found solitonlike pulses in 101 shots. We have measured the distribution of soliton heights and delay times.

Solitons in stimulated Raman scattering (SRS) were first observed in 1983 in CO₂-pumped para-H₂.¹ Although their origin was not fully understood at the time, theoretical studies¹⁻⁵ indicated that a π -phase shift in the Stokes beam could initiate the formation of the soliton. To test this conjecture, electro-optic π phase shifts were experimentally⁶ put into the Stokes beam to induce soliton formation, but surprisingly the height of the solitons was found to be highly variable.

Recent experiments⁷ on Raman scattering with visible lasers have shown that quantum fluctuations can lead to frequency variations within the gain narrowed Raman linewidth in a Raman generator. Based on Druhl's⁸ prediction that detuning will lead to soliton decay, it was then suggested⁷ that these frequency variations might explain the variation in soliton heights seen experimentally. Experiments performed recently⁹ with visible lasers have measured the distribution of heights of solitons initiated by electro-optic π phase shifts and compared this distribution to the predictions of soliton decay due to detuning. The qualitative agreement suggests that the decay of solitons induced by electro-optic phase shifts is indeed related to frequency variations caused by quantum fluctuations.

Englund and Bowden^{10,11} have predicted that quantum fluctuations also play a role in the generation of spontaneous solitons in SRS. However, in this case the phase shifts that lead to solitons originate from initiating quantum fluctuations. In fact it appears that these macroscopic spontaneous solitons will provide a means to study the quantum fluctuations important in the initiation of the Stokes pulse. Recently Englund and Bowden have calculated the expected distribution of fractional heights of these spontaneous solitons.¹² The theory of coherent modes¹³ also predicts that π phase shifts occur occasionally, and will therefore lead to spontaneous solitons. However, a quantitative prediction of the soliton distribution has not been made. Recently, Raymer, Li, and Walmsley¹⁴ have studied temporal quantum fluctuations emphasizing the occasional formation of a π phase shift.

In this Rapid Communication we present the results from our measurements of these spontaneous solitons, including the distribution of fractional heights of the solitons and the temporal position of the spontaneous solitons in the depletion region. We then compare our findings with the calculations of Englund and Bowden.

Figure 1 diagrams the apparatus used in the experiment. The pump laser was a single-mode, frequency-

doubled Nd:YAG pulsed laser with a nearly Gaussian 20-ns full width at half maximum (FWHM) pulse at 532 nm. The Raman scattering took place in a cell of 10-atm hydrogen gas,¹⁵ and was done on the vibrational $Q_{01}(1)$ transition at room temperature. The Raman medium of hydrogen gas was placed in a multipass cell to enhance the gain and reduce competing effects such as backward-Stokes, second-Stokes, and anti-Stokes generation.¹⁶ The fifteen passes in the multipass cell gave a gain enhancement of 12.4 over the single-pass geometry. The input pump-pulse energy was set to approximately 1 mJ, which gave enough gain that the growth of the Stokes beam from quantum initiation led to substantial pump depletion. Because there were shot-to-shot variations due to the pointing accuracy of the pump laser, the input pump beam was also put through a multipass cell before measuring its temporal profile.

Both the input and output pump beams were monitored with fast photodiodes to obtain their temporal profiles. Figure 2 shows a typical temporal profile of the depleted pump with the input pump (dashed curve) included for comparison. The forming soliton pulse is seen in the center of the pump depletion region. The fast photodiodes have a rise time of 500 ps, and the signals were recorded on 500-MHz oscilloscopes which gave an overall time resolution of 0.81 ns (FWHM).⁹ The solitons observed

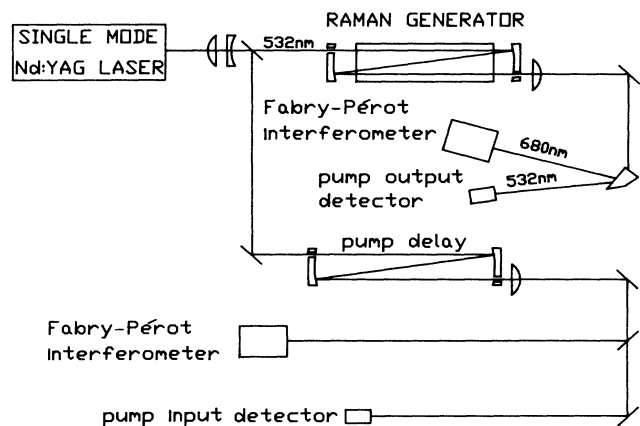


FIG. 1. Experimental apparatus used to study spontaneous solitons. The solitons were detected as pulses forming in the region of depletion in the output pump.

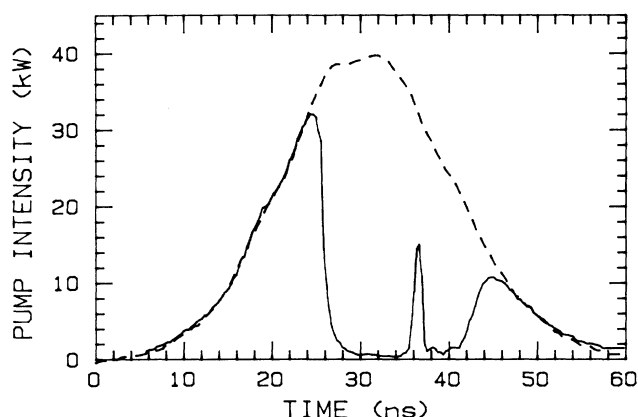


FIG. 2. A typical spontaneous soliton in the depletion region of the output pump pulse. The input pump is shown for comparison. The soliton shown has a fractional height of 0.46 and a soliton delay time of 0.60.

had widths which varied from 1.1 to 1.7 ns depending on the amount of pump depletion¹⁷ and on where in the pump depletion region the soliton occurred.

In addition to the temporal monitor, the output Stokes beam was passed through a Fabry-Pérot interferometer to obtain its power spectrum for each shot, so any correlation with spontaneous soliton formation could be studied. A second Fabry-Pérot interferometer was used to monitor a portion of the pump beam to insure that data were taken only during periods of pump stability. Both Fabry-Pérot interferometers used in the experiment had a finesse of approximately 70 and a resolution of 15 MHz. The Stokes beams was expanded and passed through one of the Fabry-Pérot interferometers with the divergence adjusted to obtain two orders of rings. A cross section of the rings was sampled by focusing them onto a photodiode array. Using a computer that was interfaced to the photodiode array we took a power-spectrum measurement of each shot.

We recorded the temporal profile, as in Fig. 2, for 1000 shots to study the statistics of the spontaneous soliton formation. For each of these shots we measured the fractional height of the solitons observed. The fractional height of the soliton was defined as the height of the soliton measured from its base, divided by its maximum possible height as measured from the input pump. The soliton shown in Fig. 2 had a fractional height of 0.46. Out of 1000 shots we observed 101 solitons with fractional heights that ranged from 0.03 to 0.82. Every shot with a soliton was photographed, several of which were digitized. The digitized input and output pulses were scaled to match in the temporal wings. The average of the scale factor for the shots that were digitized was used to calculate fractional heights for the shots that were not digitized. From the digitized data, the scale factor was found to have an uncertainty of 9%. Only solitons that occurred in the region between the temporal half-heights of the undepleted output pump signal were recorded. Occasional shots with regions of pump depletion greater than 25 ns or less than 15 ns were not included in the data.

The distribution of fractional heights for the 101 solitons observed is shown in Fig. 3 in a histogram. As can be seen from the figure, spontaneous solitons of small fractional heights are most probable with the distribution tapering off at large fractional heights. Interestingly, this distribution is almost the mirror image of the distribution measured⁹ with electro-optically induced π phase shifts in a Stokes seed to a Raman amplifier. Even for the electro-optically induced π phase shifts, not all solitons were of full height because of detuning-induced soliton decay. Nonetheless, in that case the most probable fractional height was still near full amplitude. However, for the spontaneous solitons reported here, the deviation of the quantum noise-induced phase shift from π also leads to lower fractional heights which skews the distribution to the lower values as seen in Fig. 3.

Englund and Bowden¹² have calculated the distribution of soliton fractional heights and find that above a fractional height of 0.2, the distribution was fairly uniform as opposed to our distribution shown in Fig. 3, which tapers off at large heights. This difference may be due to the finite rise time of our detector which will skew the distribution to low values. Future calculations will probably need to include this response time for a detailed comparison with experiment. The prediction for the total number of solitons above a fractional height of 0.2 at a pressure comparable to that of the experiment was 211 in an ensemble of 10000 or 2.1%. If we count only solitons above a fractional height of 0.2 for our data, we obtain (from Fig. 3) 38 solitons in an ensemble of 1000 or 3.8% which is higher than predicted. However, for an accurate comparison, a calculation will have to be done for the specific pulse length and amount of pump depletion observed in the experiment.

We also studied the spectrum of the Stokes beam to see any correlations with the spontaneous soliton formation. Clearly, the power spectrum of a pulse with a π phase change in it has to have more structure than one with little or no phase structure. As might be expected, the Stokes power spectrum of each shot with a spontaneous soliton was observed to have more structure than most of those

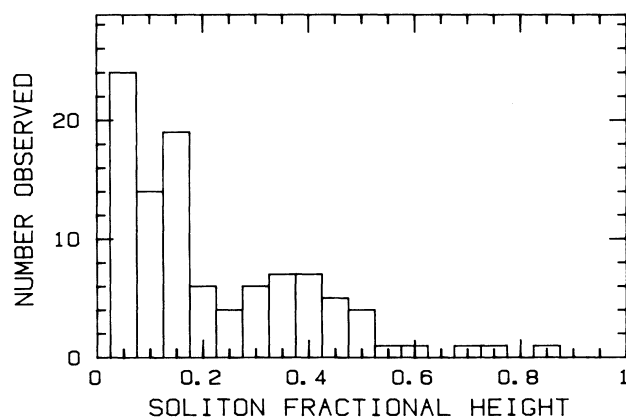


FIG. 3. Distribution of spontaneous soliton fractional heights. From the 1000 shots we observed 101 spontaneous solitons with heights of 0.03 or larger.

without solitons, some showing distinctive double peaks. Conversely, a few shots with considerable structure on the Stokes power spectrum did not exhibit solitons. One possible explanation for this could be that the initiating quantum phase shift was too complex to yield the abrupt π shift needed to generate a soliton.

In Fig. 4 we show a histogram of the number of solitons observed as a function of the soliton delay time in relative units. The soliton delay time was taken to be the fraction of the time from the beginning of the pump depletion region to the soliton, divided by the duration of the pump depletion. For example, in Fig. 2 the pump depletion starts at 25 ns and ends at 45 ns, giving a duration of 20 ns. The soliton in Fig. 2 occurred at 37 ns, 12 ns from the beginning of pump depletion. Thus this soliton had a delay time of $12/20 = 0.60$. Since the solitons originate from random quantum fluctuations we expected the distribution shown in Fig. 4 to be uniform. However, preliminary calculations by Englund and Bowden¹⁸ indicate that this distribution should be peaked towards the beginning of the pump depletion region. This is qualitatively what we see in our data shown in Fig. 4. While we have no physical picture for the origin of this asymmetric distribution, clearly the evolving phase shift must be strongly influenced by the temporal gain profile of the pump laser.

Curiously, out of the 1000 shots recorded we observed only one shot with two spontaneous solitons. Since we saw single solitons in approximately one in ten shots, we expected to see double solitons in approximately one in 100 shots, or ten from our sample of 1000 shots. Thus our data indicate that the presence of one soliton may inhibit the formation of another. To test this conjecture we ran a computer simulation with the semiclassical equations for

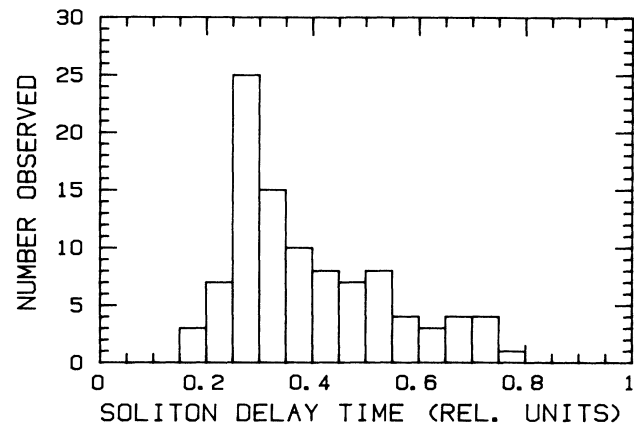


FIG. 4. Distribution of soliton delay times measured relative to the duration of the temporal depletion region.

two closely spaced π phase shifts in a Stokes seed. After amplifying the Stokes seed by approximately the same amount as spontaneous emission is amplified in the Raman generator, we found that no solitons resulted when the two phase shifts were closer than 2.5 ns apart. However, when the phase shifts were separated by 3 ns the two soliton pulses appeared to evolve independently. Thus the interaction between closely spaced solitons along with the peaked distribution shown in Fig. 4 may explain the dearth of shots with multiple solitons.

This work was supported by the National Science Foundation Grant No. PHY-8900282.

¹K. Druhl, R. G. Wenzel, and J. L. Carlsten, Phys. Rev. Lett. **51**, 1171 (1983).

²K. Druhl, J. L. Carlsten, and R. G. Wenzel, J. Stat. Phys. **36**, 615 (1985).

³K. Druhl and G. Alsing, Physica D **20**, 429 (1986).

⁴H. Steudel, Opt. Commun. **57**, 285 (1986).

⁵D. J. Kaup, Physica D **19**, 125 (1986).

⁶R. G. Wenzel, J. L. Carlsten, and K. J. Druhl, J. Stat. Phys. **39**, 621 (1985).

⁷D. C. MacPherson, R. C. Swanson, and J. L. Carlsten, Phys. Rev. Lett. **61**, 66 (1988).

⁸M. Yousaf, K. J. Druhl, and S. A. Shakir, Physica D **30**, 228 (1988).

⁹D. C. MacPherson, R. C. Swanson, and J. L. Carlsten, Phys. Rev. A **39**, 6078 (1989).

¹⁰J. C. Englund and C. M. Bowden, Phys. Rev. Lett. **57**, 2661 (1986).

¹¹C. M. Bowden and J. C. Englund, Opt. Commun. **67**, 71 (1988).

¹²J. C. Englund and C. M. Bowden, in *Nonlinear Optical Beam Manipulation. Beams Combining in Atmospheric Propagation*, SPIE Conference Proceedings No. 874 (International Society for Optical Engineering, Bellingham, WA, 1988), p. 218.

¹³D. C. MacPherson, R. C. Swanson, and J. L. Carlsten, Phys. Rev. A **39**, 3487 (1989).

¹⁴M. G. Raymer, Z. W. Li, and I. A. Walmsley, Phys. Rev. Lett. **63**, 1586 (1989).

¹⁵We have also observed spontaneous solitons in a cell of 30-atm H₂. However, due to the finite response time of our oscilloscope we chose to present the data from the experiment using 10-atm H₂ which produced broader solitons.

¹⁶D. C. MacPherson, R. C. Swanson, and J. L. Carlsten, IEEE J. Quantum Electron. **QE-25**, 1741 (1989).

¹⁷D. C. MacPherson, J. L. Carlsten, and K. J. Druhl, J. Opt. Soc. Am. B **4**, 1853 (1987).

¹⁸J. C. Englund (private communication).